

LaViP: Language-Grounded Visual Prompts

Nilakshan Kunananthaseelan¹, Jing Zhang², Mehrtash Harandi¹

¹Department of Electrical and Computer Systems Engineering, Monash University

²College of Engineering and Computer Science, Australian National University

{nilakshan.kunananthaseelan, mehrtash.harandi}@monash.edu, jing.zhang@anu.edu.au

Abstract

We introduce a language-grounded visual prompting method to adapt the visual encoder of vision-language models for downstream tasks. By capitalizing on language integration, we devise a parameter-efficient strategy to adjust the input of the visual encoder, eliminating the need to modify or add to the model’s parameters. Due to this design choice, our algorithm can operate even in black-box scenarios, showcasing adaptability in situations where access to the model’s parameters is constrained. We will empirically demonstrate that, compared to prior art, grounding visual prompts with language enhances both the accuracy and speed of adaptation. Moreover, our algorithm excels in base-to-novel class generalization, overcoming limitations of visual prompting and exhibiting the capacity to generalize beyond seen classes. We thoroughly assess and evaluate our method across a variety of image recognition datasets, such as EuroSAT, UCF101, DTD, and CLEVR, spanning different learning situations, including few-shot learning, base-to-novel class generalization, and transfer learning.

1 Introduction

Large-scale pre-trained models (PTMs) (Brown et al. 2020a; Dosovitskiy et al. 2020; Radford et al. 2021; Touvron et al. 2023; Kirillov et al. 2023) are trained on massive amounts of data and intricate optimization throughout the learning process. This makes designing and developing high-performing PTMs a laborious and costly process. While these models showcase generalization prowess, achieving optimal performance on new tasks necessitates careful finetuning. Nonetheless, the finetuning of PTMs carries inherent challenges, notably the risk of catastrophic knowledge forgetting and vulnerability to overfitting on the downstream tasks (Kumar et al. 2021; Wortsman et al. 2022).

In response to the aforementioned challenges, *model reprogramming* (MR) (Elsayed, Goodfellow, and Sohl-Dickstein 2018), a method in the context of transfer learning, has emerged as a fresh paradigm. The core idea behind MR is to repurpose and harness a high-quality pre-trained model, facilitating seamless cross-domain learning *without the need for finetuning* the model. MR introduces a learnable transformation function at the input of the model, along with

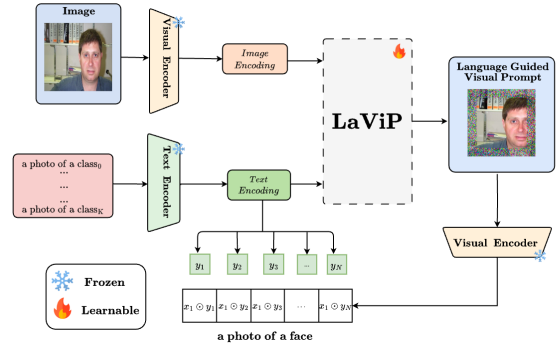


Figure 1: Our key idea is to reprogram the visual encoder of CLIP (Radford et al. 2021) through the generation of language-grounded visual prompts.

an output mapping function to achieve this objective. The pioneering work of (Tsai, Chen, and Ho 2020) has demonstrated that through MR, even a CNN initially trained on ImageNet can be swiftly adapted to excel in classifying medical images, interestingly, even outperforming the traditional finetuning approach. Subsequent research efforts have extended the idea of MR into various domains, achieving successful adaption without finetuning (Vinod, Chen, and Das 2020; Yen et al. 2021; Yang, Tsai, and Chen 2021; Neekharu et al. 2022; Chen et al. 2023).

The input transformation acquired through MR is commonly conceptualized as a perturbation pattern, which is either added to or concatenated with the input images. By learning the perturbation pattern, also called Visual Prompts (VPs) in vision tasks, the PTM effectively embeds the downstream task samples into a distinct subset of its latent space. As such, MR allows to adeptly repurpose the PTM’s capabilities, all while preserving the integrity of the latent space. Despite the promise and rapid progress, several questions remain unanswered in MR;

- **Unimodality in learning VPs.** To the best of our knowledge, in the previous studies focusing on VPs, class semantic information and visual encoding are typically treated separately in many cases, despite human perception being multimodal (e.g., (Gibson 1969; Meltzoff

and Borton 1979; Quiroga et al. 2005). This multimodal framework of our cognitive system helps us to learn new concepts with a few examples. This, in AI, will raise a simple question, *if a Vision-Language model is at hand, does language help in designing VPs for MR? If yes, what are the design questions to answer?*

- **Efficient Training.** In practice, learning VPs require a large number of iterations to achieve quality results. *For example, adapting a PTM to classify 10 classes of satellite images in EuroSAT (Helber et al. 2019a), requires 1000 training epochs.* This is because, adapting the visual encoder is challenging due to the complexity of high-dimensional visual input and the asymmetric nature of V-L encoders, compared to its text counterpart. One may wonder whether language can overcome this constraint.
- **Generalizing beyond seen classes.** MR is, by nature, a form of transfer learning. As such, it does not endow an explicit mechanism to generalize beyond what it has seen during adaptation. Recent studies have shown that Vision Language Models (VLMs) have great zero-shot learning capabilities. This would suggest whether one can expect or design an MR algorithm that can benefit from language to generalize beyond its seen classes during adaptation.
- **Adaptation without accessing model parameters** Our method maintains the original foundation model, thus enabling adaptation via APIs and cases where for ethical constraints, accessing the structure and weights of the foundation model is not possible. Furthermore, preserving the foundation model translates into maintaining its generalization capabilities, a virtue, that algorithms such as MaPLe (Khattak et al. 2023) cannot ensure.

Our work takes a stride toward addressing the aforementioned questions. In particular, we propose **Language-Grounded Visual Prompting (LaViP)**¹, which enables pixel-space input-aware prompting by leveraging the language integration to adapt downstream tasks (Figure 1). In LaViP, we opt for a low-rank solution to generate language grounded visual prompt. This substantially reduces the number of parameters to be learned, a quality particularly advantageous in the context of black-box settings. Furthermore, we develop a mechanism to incorporate novel class knowledge without needing to retrain the VPs, enabling our solution to generalize to novel and unseen classes seamlessly. To contrast and compare our algorithm against previous art, we have performed a thorough set of experiments, ranging over transfer learning, few-shot learning, and generalization beyond seen classes over 12 recognition datasets. Our empirical study shows that our algorithm consistently outperforms state-of-the-art algorithms by a tangible margin by harnessing the multimodal signals in visual prompts.

To summarize, we have made the following contributions to this work. Firstly, to the best of our knowledge, we are pioneering a language-grounded MR solution to adapt a visual encoder to downstream tasks. Secondly, we propose

¹<https://github.com/NilakshanKunananthaseelan/LaViP>

a mechanism effectively extending visual prompts beyond seen classes, a feat largely confined to text prompt adaptation. We extensively evaluate and assess our algorithm on three learning paradigms: few-shot learning, generalization beyond seen classes, and transfer learning.

2 LaViP

Throughout the paper, we denote scalars as x , vectors as \mathbf{x} , matrices as \mathbf{X} , and equality by definition as \triangleq . The Kronecker product between matrix $\mathbf{X} \in \mathbb{R}^{m \times n}$ and $\mathbf{Y} \in \mathbb{R}^{p \times q}$, denoted by $\mathbf{X} \otimes \mathbf{Y} \in \mathbb{R}^{mp \times nq}$ is defined as

$$\mathbf{X} \otimes \mathbf{Y} = \begin{pmatrix} x_{11}\mathbf{Y} & \cdots & x_{1n}\mathbf{Y} \\ \vdots & \ddots & \vdots \\ x_{m1}\mathbf{Y} & \cdots & x_{mn}\mathbf{Y} \end{pmatrix}, \quad (1)$$

where a_{ij} represents the element in the i -th row and j -th column of \mathbf{X} . Below, we describe **LaViP**, our input-dependent visual prompting approach guided by language semantics. In § 2.1, we provide a detailed exposition of the underlying rationale of our algorithm and its design. § 2.2 illustrates how LaViP can be transitioned to base-to-novel generalization tasks.

Problem Statement. Given a training dataset $\mathcal{S} = \{(\mathbf{x}_i, \mathbf{y}_i)_{i=1}^m\}$ drawn i.i.d. from distribution \mathcal{D} , we seek to learn a model to effectively assign input vectors \mathbf{x} to their corresponding class labels \mathbf{y} , based on the patterns and relationships. We assume $\mathbf{x}_i \in \mathbb{R}^{\mathbb{H} \times \mathbb{W} \times \mathbb{C}}$ is an image and $\mathbf{y}_i \in \Delta^{K-1}$ is its associated label, with Δ^{K-1} denoting the K -simplex. Furthermore, we assume a pre-trained VLM with a visual encoder $\Phi_{\text{vis}} : \mathbb{R}^{\mathbb{H} \times \mathbb{W} \times \mathbb{C}} \rightarrow \mathbb{R}^d$ $\Phi_{\text{lan}} : \mathcal{X} \rightarrow \mathbb{R}^d$ is at our disposal. Here, $\mathcal{X} \subseteq \mathbb{R}^{d_t}$ denotes the input space of the language encoder, in the case of CLIP, a subset of integers defined by its tokenizer.

To achieve this goal, our objective is to generate padding-style visual prompts with a total of $2p\mathbb{C}(\mathbb{H} + \mathbb{W} - 2p)$ parameters, where \mathbb{C} represents channels, \mathbb{H} and \mathbb{W} denote height and width, and p is the padding size. Unlike previous visual prompting methods such as VP (Bahng et al. 2022), LaViP adopts an approach where it learns input-specific prompts that are language-grounded.

2.1 Language Grounded Visual Prompts

Visual Prompts manipulate the pixel space via learnable parameters and steer the PTMS in any desired direction. While VP made the first contribution to this concept in the context of the pre-trained vision model and VLMs, they overlooked 1) the multimodal nature of VLMs, and 2) the semantic diversity of images. To address these gaps, we propose LaViP, a novel approach that capitalizes on these two important observations. Figure 2 provides an overview of our method. LaViP synergizes complex intricacies in inputs and context expertise, generating language-grounded input-aware visual prompts, which facilitates enhanced modality alignment.

As suggested earlier, the visual prompt for a sample $\mathbf{x} \in \mathbb{R}^{\mathbb{H} \times \mathbb{W} \times \mathbb{C}}$ is defined as $\boldsymbol{\nu} \in \mathbb{R}^{2\mathbb{C}(\mathbb{H} + \mathbb{W} - 2p)p}$, which is padded around a resized version of \mathbf{x} . We mathematically and with

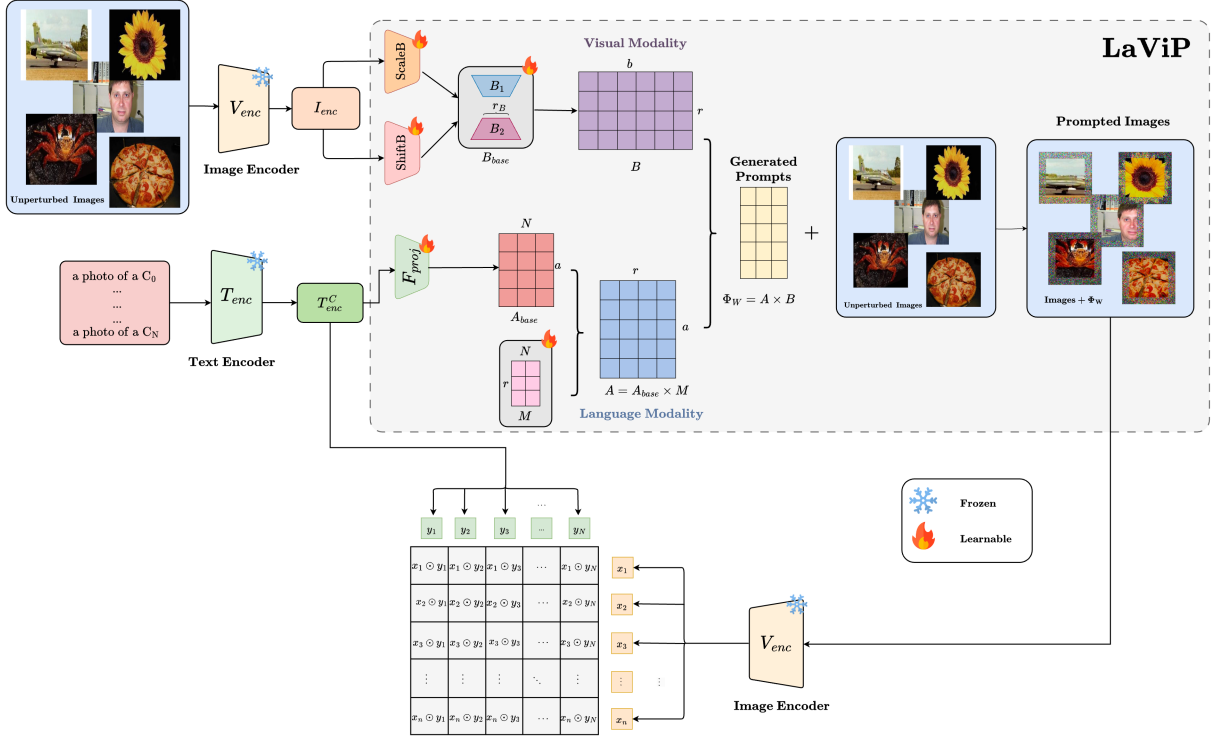


Figure 2: Overview of our proposed Language-Grounded Visual Prompting(LaViP) for VLMs: LaViP utilizes language-grounded input-specific visual programs to reprogram the frozen visual encoder of the CLIP model. LaViP scales and shifts local image encoding and projects global text encoding. The subsequent matrix multiplication of these localized and global projections fosters a mutual synergy between the two modalities, resulting in the generation of adaptive visual prompts.

a bit of abuse of notation show this process by:

$$\tilde{\mathbf{x}} = \mathbf{x} \oplus \boldsymbol{\nu}. \quad (2)$$

For a VLM such as CLIP, typical values of $H = W = 224$, and $p = 28$, which results in generating $2C(H + W - 2p)p$ parameters for VPs.

We aim to facilitate the generation of input-specific visual prompts by formulating the process through low-rank matrix decomposition. Specifically, we derive two matrices $\mathbf{A} \in \mathbb{R}^{a \times r}$, $\mathbf{B} \in \mathbb{R}^{r \times b}$ and $\mathbf{M} \in \mathbb{R}^{K \times r}$. Here, \mathbf{A} acts as a projection and captures the class semantics of the problem via the language encoder. Furthermore and as we will show shortly, \mathbf{A} is obtained from the textual description of all K classes. This implies that after training, our algorithm can only store \mathbf{A} and does not need a language encoder to operate in its nominal form.

On the other hand, the \mathbf{B} component of the VP is tailored to each image, enabling our method, LaViP, to dynamically adjust its prompts based on the input image it receives. This image dependency aligns with the idea that customized guidance can enhance model performance, as previously discussed. We argue that, despite sharing identical class labels, images often exhibit distinct semantic variations. Relying on

universal visual prompts limits the model’s capacity to adapt effectively to these variations, especially when extending to unseen classes. The hyper-parameter r controls the rank of \mathbf{A} and \mathbf{B} , and can be considered as a prior in generating VPs. Consequently, we represent the VP as $\boldsymbol{\nu} = \text{Vec}(\mathbf{A}\mathbf{B})$. Here, the notation $\text{Vec}(\cdot)$ denotes the process of reshaping a matrix into a vector. By adopting this formulation, we reduce the complexity of requiring $\boldsymbol{\nu}$ from the initially required $2C(H + W - 2p)p$ parameters to merely $r(a + b)$ parameters for each instance. Learning low-rank decomposition of learnable parameters has proven more effective and efficient than finetuning all parameters (Hu et al. 2021). Below, we provide a detailed explanation of how \mathbf{A} and \mathbf{B} are generated.

Language-Grounded Encoding Following common practice (Radford et al. 2021; Bahng et al. 2022), for all K classes of a downstream, we craft textual descriptions by a template in the form: “a photo of a $\langle class \rangle$ ”. Then, we obtain the encoding of the VLM language coder for all K prompts as $\mathbf{T}_{\text{enc}} \in \mathbb{R}^{K \times d}$ using:

$$\mathbf{T}_{\text{enc}} = \text{VLM}_{\text{TextEncoder}}(\text{prompts}). \quad (3)$$

To enrich the representation, we define $\mathbf{A} \triangleq \mathbf{M}\mathbf{A}_{\text{base}}$.

Algorithm 1: LaViP algorithm

Input: Target dataset: \mathcal{D} with K classes and X images,
Pre-trained model: F ,
Prompt learner: P with trainable parameters.
Parameters: Parameters of P : $\mathbf{B}_1, \mathbf{B}_2, \mathbf{M}, \text{Scale}_B, \text{Shift}_B$
Output: Visual prompt: Φ_W for the target task.

- 1: Initialize Parameters: $\mathbf{B}_1, \mathbf{B}_2$ and \mathbf{M}
 - 2: Create Visual Projection Matrix: $\mathbf{B}_{\text{base}} = \mathbf{B}_1 \times \mathbf{B}_2$
 - 3: Construct K textual prompts: $\text{prompts} = \{ \text{a photo of a } \{i\}_{i=1}^K \}$
 - 4: Encode the image and text prompt:
 $T_{\text{enc}}, I_{\text{enc}} = F(x, \text{prompts})$
 - 5: Project text encoding: $\mathbf{A}_{\text{base}} = f(T_{\text{enc}})$
 - 6: Control the text integration: $\mathbf{A} = \mathbf{M} \times \mathbf{A}_{\text{base}}$
 - 7: Scaling and shifting of image encoding:
 $\mathbf{B}_{\text{scale}} = \text{Scale}_B(I_{\text{enc}})$
 $\mathbf{B}_{\text{shift}} = \text{Shift}_B(I_{\text{enc}})$
 - 8: Feature-wise modulation:
 $\mathbf{B} \triangleq \mathbf{B}_{\text{scale}} \odot \mathbf{B}_{\text{base}} + \mathbf{B}_{\text{shift}}$
 - 9: Combine the textual and image-specific information :
 $\Phi_W = \mathbf{A} \times \mathbf{B}$
-

Here, \mathbf{A}_{base} is obtained from the semantics T_{enc} (see Eq.(3)) as $\mathbf{A}_{\text{base}} = f(T_{\text{enc}})$. The matrix \mathbf{M} is learnable, helping the model to gauge the semantics to be incorporated as a part of VPs.

Image-dependent Encoding Similar in concept, we formulate the image-dependent part of the VP as a matrix decomposition, albeit with some touch-ups. In particular, we propose the following form for constructing \mathbf{B} :

$$\mathbf{B} \triangleq \mathbf{B}_{\text{scale}} \odot \mathbf{B}_{\text{base}} + \mathbf{B}_{\text{shift}}, \quad (4)$$

where $\mathbf{B}_{\text{scale}}, \mathbf{B}_{\text{shift}} \in \mathbb{R}^r$, $\mathbf{B}_{\text{base}} \in \mathbb{R}^{b \times r}$ and \odot indicates scaling function. In Eq.(4), \mathbf{B}_{base} is a matrix encoding the visual aspects of the input image and is obtained as:

$$\mathbf{B}_{\text{base}} = \mathbf{B}_1 \times \mathbf{B}_2, \quad (5)$$

where \mathbf{B}_1 and \mathbf{B}_2 are low-rank decomposition of \mathbf{B}_{base} with rank r_B . We modulate \mathbf{B}_{base} with $\mathbf{B}_{\text{scale}}$ and $\mathbf{B}_{\text{shift}}$, which are light-way matrices obtained through simple linear layers. We opt for light-design choices to accelerate image-wise transformation in Eq.(4) without introducing significant computational overhead and provide a convenient way to introduce non-linearity in the process. Algorithm 1 summarizes the steps involved in our method.

2.2 Generalization from Base to Novel Classes

In the base-to-novel generalization task, the goal is to evaluate the *generalizability of the model to unseen classes* by training on base classes while evaluating on the base and novel classes *separately* (Zhou et al. 2022a).

CoOp (Zhou et al. 2022b) learns text prompts neglecting input differences, therefore failing to generalize well beyond classes in training data. To alleviate such drawbacks, Co-CoOp (Zhou et al. 2022a) proposes image-conditioned text

prompts to impute novel class knowledge into prompts, and MaPLe (Khattak et al. 2023) injects tokens in both the vision and language branches which efficiently transition the novel class knowledge into prompts. In contrast to these approaches, visual prompt-based techniques lack an efficient means to integrate novel class knowledge.

We address this limitation by embedding novel-class knowledge into the visual prompts on the fly and without the need for retraining. The Kronecker product encapsulates information, eliminating the necessity for additional learning (Gao, Wang, and Ji 2020; Schwartz, Haley, and Tyers 2022; Demir, Lienen, and Ngonga Ngomo 2022; Jin, Kolda, and Ward 2021). The underlying idea is to employ the similarity between novel classes and base classes to refine \mathbf{A} . Recall that $\mathbf{A} = \mathbf{M} \mathbf{A}_{\text{base}}$. This can be understood as \mathbf{A} being a linear combination of the semantic information captured in \mathbf{A}_{base} . In the presence of novel classes, we first encode a notion of similarity between base and novel classes by

$$\mathbf{T}_{\text{enc}}^{\text{K}_{\text{novel}}} \otimes \mathbf{A} = \begin{pmatrix} t_{11}\mathbf{A} & \cdots & t_{1d}\mathbf{A} \\ \vdots & \ddots & \vdots \\ t_{K_{\text{novel}}1}\mathbf{A} & \cdots & t_{K_{\text{novel}}d}\mathbf{A} \end{pmatrix}, \quad (6)$$

where \otimes denotes the Kronecker product.

The resulting product will exist in $\mathbb{R}^{(aK_{\text{novel}}) \times (rd)}$, representing the projection of each novel class on all the base classes. To obtain a compact and coherent embedding representation between base and novel classes, we transform this class-wise projection into $\mathbb{R}^{a \times K_{\text{novel}} \times r \times d}$. Subsequently, we compute the mean along VLM features (d) and the number of novel classes (K_{novel}). The averaging operation serves to align the base classes with a more unified representation of novel classes.

3 Related Works

In this section, first, we will introduce VLMs and their constraints for adapting to new tasks, then we will discuss existing prompt learning methods, and finally, we will explore how MR is used in repurposing PTMs for diverse domains tasks.

3.1 Pretrained Vision-Language models:

VLMs such as CLIP (Radford et al. 2021), ALIGN (Jia et al. 2021), Flamingo (Alayrac et al. 2022), Flava (Singh et al. 2022) and LiT (Zhai et al. 2022) have demonstrated exceptional performance on a variety of tasks, including few-shot and zero-shot image recognition. These models learn to align the vision-language representations on a web-scale training dataset. Although pre-trained models offer a strong foundation for a wide range of tasks, efficiently adapting them to downstream tasks is still a challenging research problem. The difficulty is exacerbated when the downstream task requires specialized context, interpretable representations, or access to the model is forbidden (Mokady, Hertz, and Bermano 2021; Jiang, Liu, and Zheng 2022; Shu et al. 2023; Maus et al. 2023). Furthermore, Kumar *et al.* showed

Method	Caltech	Pets	Cars	Flowers	Food	Aircraft	SUN	DTD	EuroSAT	RESISC	CLEVR	UCF	Avg.	Win
ZS(Radford et al. 2021)	89.3	88.9	65.6	70.4	89.2	27.1	65.2	46.0	54.1	65.5	23.4	69.8	62.75	1
VP(Bahng et al. 2022)	94.2	90.2	66.9	86.9	81.8	31.8	67.1	61.9	90.8	81.4	40.8	74.2	71.26	1
LaViP(Ours)	95.0	91.2	77.8	96.3	82.5	43.2	71.1	68.8	86.1	85.6	46.5	81.3	74.59	10

Table 1: Comparison with visual prompting method on few-shot transfer learning. LaViP learns language-driven input-aware visual prompts and exhibits robust performance on 10 in 12 recognition datasets with training accelerated by *more than* $3\times$. *Win* indicates how many cases LaViP outperforms previous methods.

finetuning overparameterized models can yield detrimental results compared to linear probing (i.e., tuning the head while keeping lower layers frozen) when addressing out-of-distribution downstream tasks (Kumar et al. 2021).

3.2 Prompt Learning in VLMs

Standard finetuning and linear probing are common approaches to adapting VLMs to downstream tasks. However, such finetuning causes detrimental results due to the loss of embedded knowledge and poor adaptation techniques (Wortsman et al. 2022). There is a significant body of work in natural language processing (NLP) that focuses on learning effective prompts to adapt a large language model to downstream tasks (Sanh et al. 2021; Hounsby et al. 2019; Brown et al. 2020b; Chen et al. 2022). Inspired by the success of prompt learning in NLP, several recent studies explored prompt learning methods in the context of large-scale VLMs. Visual Prompt Tuning (VPT) learns the prefix prompts in encoder layers or embedding layer (Jia et al. 2022), while (Khattak et al. 2023) proposes injection of learnable tokens in both vision and text encoder layers and couples them with a learnable function. Visual Prompting (VP) investigated input pixel space prompt tuning for pre-trained vision and VLMs (Bahng et al. 2022). VP learns a fixed input agnostic perturbation and attaches it to the original images, hence adapting a pre-trained model to new tasks without modifying the model parameters. Bar et al. uses the inpainting method as visual prompting. Context Optimization (CoOp) (Zhou et al. 2022b) optimizes a set of context vectors for the text encoder of CLIP, while Conditional Context Optimization (CoCoOp) (Zhou et al. 2022a) generalizes CoOp to unseen classes by conditioning the text prompt optimization on image instances. (Lin et al. 2023) suggests cross-modal adaptation by repurposing class names as one-shot training examples, (Lu et al. 2022) proposes an ensemble of learnable prompts. (Menon and Vondrick 2023; Zhang et al. 2023; Dunlap et al. 2022) showcase how language can be effectively employed to strengthen the adaptation of pre-trained vision models to novel domains.

We argue that generating input-agnostic prompts with unimodal knowledge is a suboptimal approach. Considering the large-scale pre-training of VLMs, prompting methods should adeptly utilize the embedded multimodal knowledge to efficiently address new tasks. Further, we underscore the importance of prompting methods being agnostic to the underlying architecture of PTMs. For instance, VPT and MaPLe have successfully adapted ViT encoders through prefix learning. However, these methods lack comprehensive

evidence of how their solutions perform across diverse backbone architectures.

3.3 Model reprogramming

By deriving motivation from adversarial attacks Elsayed, Goodfellow, and Sohl-Dickstein (2018) proposed Adversarial Reprogramming (AR) to repurpose a pre-trained model to perform on a new domain. This led to a new learning paradigm called model reprogramming (MR) for transfer learning.

We provide some notable examples below. Vinod, Chen, and Das (2020) repurposed a language model to predict biochemical sequences; Tsai, Chen, and Ho (2020) proposed BAR to reprogram an ImageNet model for complex biomedical under a black-box setting; Yen et al. (2021) used an attention-based RNN speech model for low-resource spoken command recognition; Yang, Tsai, and Chen (2021) reprogrammed a speech model for time-series prediction and Neekhara et al. (2022) reprogrammed a vision model to classify text sentences and DNA sequences. (Oh et al. 2023) extended BAR by generating input-aware visual prompts through an external encoder-decoder model for limited data recognition.

To the best of our knowledge, we are pioneering to design of language-grounded visual prompts to reprogram the visual encoder of a VLM. In contrast to previous MR methods that primarily focused on repurposing PTMs using unimodality, our contribution lies in harnessing the power of multimodality to enhance context knowledge during adaptation.

4 Results

We first provide the experimental setup in § 4.1. Next, § 4.2 presents the comparison between LaViP and previous methods. § 4.3 provides the result for the base-to-novel generalization task and § 4.4 provides the results for whole-dataset training.

4.1 Experimental Setup

We extensively evaluate LaViP capability on 12 benchmark datasets (refer Appendix B.3) under three distinct scenarios. First, its transferability in limited data settings is assessed through few-shot learning, where it learns from 16-shots for training and 4-shots for validation. Next, its generalizability is examined by evaluating its ability to learn from base classes and apply that knowledge to unseen novel classes. Finally, we use the full dataset for training, testing and validation. In this paper, we use CLIP ViT-B/16 (Radford et al.

Dataset	CLIP			CoOp			CoCoOp			MaPLe			LaViP (Ours)		
	Base	Novel	HM	Base	Novel	HM	Base	Novel	HM	Base	Novel	HM	Base	Novel	HM
Caltech101	96.84	94.00	95.40	98.00	89.81	93.73	97.96	93.81	95.84	97.74	94.36	96.02	97.63	93.45	95.49
DTD	53.24	59.90	56.37	79.44	41.18	54.24	77.01	56.00	64.85	80.36	59.18	68.16	80.05	58.01	67.27
EuroSAT	56.48	64.05	60.03	92.19	54.74	68.69	87.49	60.04	71.21	94.07	73.23	82.35	92.53	82.31	87.12
FGVCAircraft	27.19	36.29	31.09	40.44	22.30	28.75	33.41	23.71	27.74	37.44	35.61	36.50	37.25	34.03	35.57
Food101	90.10	91.22	90.66	88.33	82.26	85.19	90.70	91.29	90.99	90.71	92.05	91.38	86.19	91.28	88.66
OxfordPets	91.17	97.26	94.12	93.67	95.29	94.47	95.20	97.69	96.43	95.43	97.76	96.58	92.45	97.22	94.78
SUN397	69.36	75.35	72.23	80.60	65.89	72.51	79.74	76.86	78.27	80.82	78.70	79.75	76.47	73.25	74.82
Flowers102	72.08	77.80	74.83	97.60	59.67	74.06	94.87	71.75	81.71	95.92	72.46	82.56	96.96	76.34	85.25
UCF101	70.53	77.50	73.85	84.69	56.05	67.46	82.33	73.45	77.64	83.00	78.66	80.77	83.83	76.46	79.97
StanfordCars	63.37	74.89	68.65	78.12	60.40	68.13	70.49	73.59	72.01	72.94	74.00	73.47	73.63	74.63	74.13
Average	69.04	74.83	71.72	83.31	62.76	70.72	80.92	71.82	75.67	82.84	75.60	78.75	81.7	75.70	78.31

Table 2: Performance of LaViP on base-to-novel generalization across 10 recognition datasets. LaViP demonstrates competitive generalization performance over CoOp and CoCoOp with an absolute gain of 2.64%. HM indicates the harmonic mean of base class accuracy and novel class accuracy.

2021) for few-shot learning and base-to-novel generalization, and CLIP ViT-B/32 for whole-set training as the pre-trained VL model due to its strong zero-shot generalization capability. More details are provided in Appendix B.

4.2 Few-shot learning

Table 1 presents the performance of LaViP in a few-shot transfer setting across 12 recognition datasets. We compare our results against CLIP Zero-shot (ZS), and the previous pixel-space reprogramming method. LaViP outperforms ZS on 11 datasets, exhibiting a substantial gain of 11.84%. Additionally, when comparing to VP (Bahng et al. 2022) on 11 datasets, achieving a gain of 3.3% in performance and more than a $3\times$ faster convergence. Furthermore, Table 1 shows that when the domain shifts from generic to rare concepts, LaViP consistently demonstrates higher performance in comparison to CLIP. This highlights the effectiveness of incorporating language guidance in enhancing modality alignment, particularly in cases where concepts can be explicitly described.

4.3 Base-to-Novel Generalization

Table 2 presents the performance of LaViP in the base-to-novel generalization setting, evaluated across 10 recognition datasets. We compare LaViP against a lineup of benchmarks, including CLIP Zero-shot (ZS), CoOp, CoCoOp and MaPLe. Relative to CoCoOp, LaViP exhibits a stronger performance across both base and novel concepts, yielding absolute gains of 0.078% and 3.88% respectively. With the context-aware knowledge diffused through Kronecker product, LaViP as a strong competitor surpasses CoCoOp in 6/10 datasets and slightly trails in two datasets. When taking into account both base and novel classes, LaViP shows an absolute average gain of with gain of 2.64% compared to CoOp and CoCoOp.

MaPLe, the current SOTA has outperformed in many studied datasets. However, unlike MaPLe, other algorithms maintain the original foundation model, thus enabling adaptation via APIs and cases where for ethical constraints, accessing the structure and weights of the foundation model is not possible. Furthermore, preserving the foundation model translates into maintaining its generalization capabilities, a

virtue, that algorithms such as MaPLe cannot ensure. LaViP trailed MaPLe by only 0.44% in performance, showcasing a competitive performance and even marginally outperforming on classifying novel classes.

In comparison with CLIP on novel classes, CoCoOp improves 3/10 classes, leading to a decrease in the average novel accuracy from 74.83% to 71.82%. LaViP only improves accuracy in 2 out of 10 datasets compared to CLIP for new classes. However, it positively impacts the average accuracy, elevating it from 74.83% to 75.70%. This sustains its position as a robust competitor. CoOp exhibits limited generalization capability to novel classes, a deficiency that CoCoOp strives to address by contextualizing text prompts based on image instances, and shows substantial improvement in novel class recognition. However, it manages to outperform 2/10 base classes with a decrease in average performance of 2.39%. LaViP’s language integration exhibits competitive performance in the base class, with only a 1.4% decrease in average performance. Despite marginal improvements compared to CoCoOp, it’s vital to recognize the dissimilarity between high-dimensional, variable-rich image data and structured text. This divergence affects learning speed and effectiveness, especially with limited data. Given the complexities inherent in the visual domain, an approach must be parameter-efficient and context-aware. This dual requirement aligns with the fundamental characteristic of LaViP.

Moreover, from Table 2 we can conclude that as the domain shift increases from the pretraining dataset, LaViP exhibits increasing performance compared to CLIP, CoOp and CoCoOp. This emphasizes the impact of language context in designing visual prompts.

Method	Pets	Flowers	Food	SUN	DTD	EuroSAT	RESISC	CLEVR	UCF	Avg.
ZS	88.3	67.4	85.2	62.6	44.4	42.2	56.6	25.8	65.2	59.75
CLIP + LP	89.2	96.9	84.6	75.0	74.6	95.3	92.3	66.0	83.3	84.13
VP	85.0	70.3	78.9	60.6	57.1	96.4	84.5	81.4	66.1	75.72
LaViP(Ours)	89.6	96.7	83.2	71.5	72.9	96.3	91.0	67.0	81.9	80.99

Table 3: Performance across 9 recognition dataset using CLIP Zero-shot (ZS), Linear Probe (LP), Visual Prompting (VP) and LaViP with ViT-B/32 backbone.

4.4 Full-dataset Learning

The summarized findings of full-dataset training are presented in Table 3. To provide a comprehensive evaluation, we draw comparisons between our results and those of CLIP Zero-shot (ZS), CLIP Linear Probe (LP), and VP, all using the ViT-B/32 CLIP model with the same hyperparameters as those used in few-shot learning. It indicates that LaViP consistently outperforms VP by a notably wider margin across 7/9 recognition datasets. This substantial improvement is coupled with an optimization process that is three times more efficient. In contrast with the results obtained from CLIP Linear Probe, VP shows enhancement in 2 out of 9 datasets, albeit accompanied by an average accuracy decrease of 8.91%. Comparatively, while LaViP only enhances performance in 1 out of 9 datasets, it achieves an average accuracy drop of 3.14%. These observations highlight the robust improvements brought about by improved visual prompting of LaViP.

5 Ablation Studies

5.1 Learning in gradient-free environment

We adapt our algorithm in a gradient-free environment to understand the effectiveness of language integration. We proceed to evaluate **BlackLaViP**, the gradient-free variant of LaViP, by employing the SPSA algorithm (Spall 1992, 2000). Table 4 presents the performance of BlackLaViP on few-shot learning on 10 recognition datasets. BlackVIP (Oh et al. 2023) uses SPSA with an external model to generate input-aware prompts and exhibits effectiveness on 4 out of 10 datasets. Though BlackLaViP doesn’t outperform BlackVIP, an intriguing observation emerges from our experiment. Remarkably, BlackLaViP attains 95% of the performance of BlackVIP with a convergence rate that is over $15\times$ faster. Implementation details are provided in Appendix C.

5.2 Impact of hyperparameters (a, b, r)

VP requires generating a padding of size $\theta = 2p_{\mathcal{C}}(\mathbb{H} + \mathbb{W} - 2p)$ as the visual prompt. We propose a low-rank formulation to generate the prompt, which efficiently reduces the generator size by a factor of 4 when $r = 32$, 2 when $r = 64$, and 1.2 when $r = 96$. The parameter r (rank of matrices in generating the prompt) can be understood as an inductive bias, regularizing the design. Empirically, we observed that LaViP performed robustly if r was chosen within a reasonable range (not too small, e.g. $r \in [16, 96]$). Furthermore, LaViP robustly performs for varying (a, b) which creates padding of size $p = 20$ to $p = 50$. Additional results are provided in Appendix D.

6 Discussion

LaViP, a novel approach to visual prompting, harnesses the power of language to enhance pre-trained models without the need for invasive finetuning. By merging textual knowledge into input prompts, LaViP steers models towards desired tasks, surpassing the limitations of previous methods in both accuracy and optimization. The few-shot capability is a direct result of preserving the foundation model. By aligning

Method	Caltech	Pets	Cars	Flowers	Food	Aircraft	DTD	RESISC	UCF	SUN	Avg.
ZS(CLIP)	89.3	88.9	65.6	70.4	89.2	27.1	46.0	65.5	69.8	62.6	67.44
VP w/SPSA-GC	89.4	87.1	56.6	67.0	80.4	23.8	44.5	61.3	64.6	61.2	63.59
BAR	93.8	88.6	63.0	71.2	84.5	24.5	47.0	65.3	64.2	62.4	66.45
BlackVIP	93.7	89.7	65.6	70.6	86.6	25.0	45.2	64.5	69.1	64.7	67.47
BlackLaViP (Ours)	92.3	89.3	63.3	68.8	84.6	23.9	46.1	61.8	65.6	62.2	65.77
%	98.5	99.6	96.5	97.5	97.7	95.6	101.2	95.8	95.1	96.1	97.49

Table 4: Comparison with state-of-the-art methods on few-shot transfer learning in a black-box setting. % indicates percentage of BlackVIP score achieved with *more than* $15\times$ faster optimization.

image and text via visual prompting and without altering the latent space of the foundation model, we capitalize on the generalization capability of the model.

Its versatility shines across diverse tasks, requiring no individual finetuning efforts, and its privacy-preserving nature makes it ideal for interacting with APIs and proprietary software. The reprogramming methodology studied in this can work to provide increased user control over bias and fairness issues in pretraining. However, low-resolution images and highly diverse datasets present challenges. We hypothesize that the observed characteristic is due to context tokens failing to grasp semantic content or capture the full spectrum of classes. LaViP’s performance is inherently influenced by the context tokens present in the prompt template. This naturally gives rise to the question: *What advantages does learning text prompts offer in comparison to employing manually crafted templates in LaViP?* Future research could delve into the direction of learning multimodal prompts with mutual synergy.

7 Conclusion

Adapting large-scale VLMs(e.g. CLIP (Radford et al. 2021)) for new tasks is a challenging research problem due to a large number of tunable parameters. Despite stemming from distinct motivation, prompt learning and model reprogramming provide an efficient and scalable approach to drive VLMs to downstream tasks. To this end, existing visual prompting approaches learn input-agnostic prompts through unimodal knowledge. The perceptual diversity of the image domain makes a difficult to repurpose visual encoders in VLMs compared to text encoders, and these approaches require an external world model to provide context or a large number of iterations. Our work counters these assumptions by leveraging embedded multimodal knowledge within VLMs. Our approach seamlessly integrates these multimodal representations to generate adaptable visual prompts, thereby enhancing performance without compromising. Further, we propose an efficient strategy for generalizing visual prompting methods to unseen classes. Our method improves the few-shot transfer learning, generalization towards novel concepts and full-set transfer learning with varying domain shifts compared to the pretraining dataset.

References

Alayrac, J.-B.; Donahue, J.; Luc, P.; Miech, A.; Barr, I.; Hasson, Y.; Lenc, K.; Mensch, A.; Millican, K.; Reynolds, M.; Ring, R.;

- Rutherford, E.; Cabi, S.; Han, T.; Gong, Z.; Samangooei, S.; Monteiro, M.; Menick, J.; Borgeaud, S.; Brock, A.; Nematzadeh, A.; Sharifzadeh, S.; Binkowski, M.; Barreira, R.; Vinyals, O.; Zisserman, A.; and Simonyan, K. 2022. Flamingo: a Visual Language Model for Few-Shot Learning. *ArXiv*, abs/2204.14198. 4
- Bahng, H.; Jahanian, A.; Sankaranarayanan, S.; and Isola, P. 2022. Exploring visual prompts for adapting large-scale models. *arXiv preprint arXiv:2203.17274*. 2, 3, 5, 6, 11
- Bar, A.; Gandelsman, Y.; Darrell, T.; Globerson, A.; and Efros, A. 2022. Visual prompting via image inpainting. *Advances in Neural Information Processing Systems*, 35: 25005–25017. 5
- Bossard, L.; Guillaumin, M.; and Van Gool, L. 2014. Food-101—mining discriminative components with random forests. In *Computer Vision—ECCV 2014: 13th European Conference, Zurich, Switzerland, September 6–12, 2014, Proceedings, Part VI 13*, 446–461. Springer. 11
- Brown, T.; Mann, B.; Ryder, N.; Subbiah, M.; Kaplan, J. D.; Dhariwal, P.; Neelakantan, A.; Shyam, P.; Sastry, G.; Askell, A.; et al. 2020a. Language models are few-shot learners. *Advances in neural information processing systems*, 33: 1877–1901. 1
- Brown, T.; Mann, B.; Ryder, N.; Subbiah, M.; Kaplan, J. D.; Dhariwal, P.; Neelakantan, A.; Shyam, P.; Sastry, G.; Askell, A.; et al. 2020b. Language models are few-shot learners. *Advances in neural information processing systems*, 33: 1877–1901. 5
- Chen, A.; Yao, Y.; Chen, P.-Y.; Zhang, Y.; and Liu, S. 2023. Understanding and improving visual prompting: A label-mapping perspective. In *Proceedings of the IEEE/CVF Conference on Computer Vision and Pattern Recognition*, 19133–19143. 1
- Chen, Y.; Liu, Y.; Dong, L.; Wang, S.; Zhu, C.; Zeng, M.; and Zhang, Y. 2022. Adaprompt: Adaptive model training for prompt-based nlp. *arXiv preprint arXiv:2202.04824*. 5
- Cheng, G.; Han, J.; and Lu, X. 2017. Remote sensing image scene classification: Benchmark and state of the art. *Proceedings of the IEEE*, 105(10): 1865–1883. 11
- Cimpoi, M.; Maji, S.; Kokkinos, I.; Mohamed, S.; and Vedaldi, A. 2014. Describing textures in the wild. In *Proceedings of the IEEE conference on computer vision and pattern recognition*, 3606–3613. 11
- Demir, C.; Lienen, J.; and Ngonga Ngomo, A.-C. 2022. Kronecker Decomposition for Knowledge Graph Embeddings. In *Proceedings of the 33rd ACM Conference on Hypertext and Social Media, HT '22*, 1–10. New York, NY, USA: Association for Computing Machinery. ISBN 9781450392334. 4
- Deng, J.; Dong, W.; Socher, R.; Li, L.-J.; Li, K.; and Fei-Fei, L. 2009. Imagenet: A large-scale hierarchical image database. In *2009 IEEE conference on computer vision and pattern recognition*, 248–255. Ieee. 14
- Dosovitskiy, A.; Beyer, L.; Kolesnikov, A.; Weissenborn, D.; Zhai, X.; Unterthiner, T.; Dehghani, M.; Minderer, M.; Heigold, G.; Gelly, S.; et al. 2020. An image is worth 16x16 words: Transformers for image recognition at scale. *arXiv preprint arXiv:2010.11929*. 1, 11
- Dunlap, L.; Mohri, C.; Guillory, D.; Zhang, H.; Darrell, T.; Gonzalez, J. E.; Raghunathan, A.; and Rohrbach, A. 2022. Using language to extend to unseen domains. In *The Eleventh International Conference on Learning Representations*. 5
- Elsayed, G. F.; Goodfellow, I.; and Sohl-Dickstein, J. 2018. Adversarial reprogramming of neural networks. *arXiv preprint arXiv:1806.11146*. 1, 5
- Fei-Fei, L.; Fergus, R.; and Perona, P. 2004. Learning generative visual models from few training examples: An incremental bayesian approach tested on 101 object categories. In *2004 conference on computer vision and pattern recognition workshop*, 178–178. IEEE. 11
- Gao, H.; Wang, Z.; and Ji, S. 2020. Kronecker attention networks. In *Proceedings of the 26th ACM SIGKDD International Conference on Knowledge Discovery & Data Mining*, 229–237. 4
- Gibson, E. J. 1969. Principles of perceptual learning and development. 1
- Helber, P.; Bischke, B.; Dengel, A.; and Borth, D. 2019a. Eurosat: A novel dataset and deep learning benchmark for land use and land cover classification. *IEEE Journal of Selected Topics in Applied Earth Observations and Remote Sensing*. 2
- Helber, P.; Bischke, B.; Dengel, A.; and Borth, D. 2019b. Eurosat: A novel dataset and deep learning benchmark for land use and land cover classification. *IEEE Journal of Selected Topics in Applied Earth Observations and Remote Sensing*, 12(7): 2217–2226. 11
- Houlsby, N.; Giurgiu, A.; Jastrzebski, S.; Morrone, B.; De Larousilhe, Q.; Gesmundo, A.; Attariyan, M.; and Gelly, S. 2019. Parameter-efficient transfer learning for NLP. In *International Conference on Machine Learning*, 2790–2799. PMLR. 5
- Hu, E. J.; Shen, Y.; Wallis, P.; Allen-Zhu, Z.; Li, Y.; Wang, S.; Wang, L.; and Chen, W. 2021. Lora: Low-rank adaptation of large language models. *arXiv preprint arXiv:2106.09685*. 3
- Jia, C.; Yang, Y.; Xia, Y.; Chen, Y.-T.; Parekh, Z.; Pham, H.; Le, Q.; Sung, Y.-H.; Li, Z.; and Duerig, T. 2021. Scaling up visual and vision-language representation learning with noisy text supervision. In *International conference on machine learning*, 4904–4916. PMLR. 4
- Jia, M.; Tang, L.; Chen, B.-C.; Cardie, C.; Belongie, S.; Hariharan, B.; and Lim, S.-N. 2022. Visual Prompt Tuning. In *European Conference on Computer Vision (ECCV)*. 5
- Jiang, J.; Liu, Z.; and Zheng, N. 2022. Finetuning pre-trained vision-language models with correlation information bottleneck for robust visual question answering. *arXiv preprint arXiv:2209.06954*. 4
- Jin, R.; Kolda, T. G.; and Ward, R. 2021. Faster johnson–lindenstrauss transforms via kronecker products. *Information and Inference: A Journal of the IMA*, 10(4): 1533–1562. 4
- Johnson, J.; Hariharan, B.; Van Der Maaten, L.; Fei-Fei, L.; Lawrence Zitnick, C.; and Girshick, R. 2017. Clevr: A diagnostic dataset for compositional language and elementary visual reasoning. In *Proceedings of the IEEE conference on computer vision and pattern recognition*, 2901–2910. 11
- Khattak, M. U.; Rasheed, H.; Maaz, M.; Khan, S.; and Khan, F. S. 2023. MaPLe: Multi-Modal Prompt Learning. In *Proceedings of the IEEE/CVF Conference on Computer Vision and Pattern Recognition (CVPR)*, 19113–19122. 2, 4, 5
- Kirillov, A.; Mintun, E.; Ravi, N.; Mao, H.; Rolland, C.; Gustafson, L.; Xiao, T.; Whitehead, S.; Berg, A. C.; Lo, W.-Y.; et al. 2023. Segment anything. *arXiv preprint arXiv:2304.02643*. 1
- Krause, J.; Stark, M.; Deng, J.; and Fei-Fei, L. 2013. 3d object representations for fine-grained categorization. In *Proceedings of the IEEE international conference on computer vision workshops*, 554–561. 11
- Krizhevsky, A.; Hinton, G.; et al. 2009. Learning multiple layers of features from tiny images. 11
- Kumar, A.; Raghunathan, A.; Jones, R. M.; Ma, T.; and Liang, P. 2021. Fine-Tuning can Distort Pretrained Features and Underperform Out-of-Distribution. In *International Conference on Learning Representations*. 1, 5

- Lin, Z.; Yu, S.; Kuang, Z.; Pathak, D.; and Ramanan, D. 2023. Multimodality helps unimodality: Cross-modal few-shot learning with multimodal models. In *Proceedings of the IEEE/CVF Conference on Computer Vision and Pattern Recognition*, 19325–19337. [5](#)
- Lu, Y.; Liu, J.; Zhang, Y.; Liu, Y.; and Tian, X. 2022. Prompt Distribution Learning. In *Proceedings of the IEEE/CVF Conference on Computer Vision and Pattern Recognition (CVPR)*, 5206–5215. [5](#)
- Maji, S.; Rahtu, E.; Kannala, J.; Blaschko, M.; and Vedaldi, A. 2013. Fine-grained visual classification of aircraft. *arXiv preprint arXiv:1306.5151*. [11](#)
- Maus, N.; Chao, P.; Wong, E.; and Gardner, J. 2023. Adversarial prompting for black box foundation models. *arXiv preprint arXiv:2302.04237*. [4](#)
- Meltzoff, A. N.; and Borton, R. W. 1979. Intermodal matching by human neonates. *Nature*, 282(5737): 403–404. [1](#)
- Menon, S.; and Vondrick, C. 2023. Visual Classification via Description from Large Language Models. *ICLR*. [5](#)
- Mokady, R.; Hertz, A.; and Bermano, A. H. 2021. Clipcap: Clip prefix for image captioning. *arXiv preprint arXiv:2111.09734*. [4](#)
- Neeckhara, P.; Hussain, S.; Du, J.; Dubnov, S.; Koushanfar, F.; and McAuley, J. 2022. Cross-modal adversarial reprogramming. In *Proceedings of the IEEE/CVF Winter Conference on Applications of Computer Vision*, 2427–2435. [1](#), [5](#)
- Netzer, Y.; Wang, T.; Coates, A.; Bissacco, A.; Wu, B.; and Ng, A. Y. 2011. Reading digits in natural images with unsupervised feature learning. [11](#)
- Nilsback, M.-E.; and Zisserman, A. 2008. Automated flower classification over a large number of classes. In *2008 Sixth Indian conference on computer vision, graphics & image processing*, 722–729. IEEE. [11](#)
- Oh, C.; Hwang, H.; Lee, H.-y.; Lim, Y.; Jung, G.; Jung, J.; Choi, H.; and Song, K. 2023. BlackVIP: Black-Box Visual Prompting for Robust Transfer Learning. In *Proceedings of the IEEE/CVF Conference on Computer Vision and Pattern Recognition*, 24224–24235. [5](#), [7](#), [11](#)
- Parkhi, O. M.; Vedaldi, A.; Zisserman, A.; and Jawahar, C. 2012. Cats and dogs. In *2012 IEEE conference on computer vision and pattern recognition*, 3498–3505. IEEE. [11](#)
- Quiroga, R. Q.; Reddy, L.; Kreiman, G.; Koch, C.; and Fried, I. 2005. Invariant visual representation by single neurons in the human brain. *Nature*, 435(7045): 1102–1107. [2](#)
- Radford, A.; Kim, J. W.; Hallacy, C.; Ramesh, A.; Goh, G.; Agarwal, S.; Sastry, G.; Askell, A.; Mishkin, P.; Clark, J.; et al. 2021. Learning transferable visual models from natural language supervision. In *International conference on machine learning*, 8748–8763. PMLR. [1](#), [3](#), [4](#), [5](#), [7](#), [10](#), [11](#)
- Sanh, V.; Webson, A.; Raffel, C.; Bach, S. H.; Sutawika, L.; Alyafeai, Z.; Chaffin, A.; Stiegler, A.; Scao, T. L.; Raja, A.; et al. 2021. Multitask prompted training enables zero-shot task generalization. *arXiv preprint arXiv:2110.08207*. [5](#)
- Schwartz, L.; Haley, C.; and Tyers, F. 2022. How to encode arbitrarily complex morphology in word embeddings, no corpus needed. In *Proceedings of the first workshop on NLP applications to field linguistics*, 64–76. Gyeongju, Republic of Korea: International Conference on Computational Linguistics. [4](#)
- Shu, Y.; Guo, X.; Wu, J.; Wang, X.; Wang, J.; and Long, M. 2023. CLIPood: Generalizing CLIP to Out-of-Distributions. In Krause, A.; Brunskill, E.; Cho, K.; Engelhardt, B.; Sabato, S.; and Scarlett, J., eds., *Proceedings of the 40th International Conference on Machine Learning*, volume 202 of *Proceedings of Machine Learning Research*, 31716–31731. PMLR. [4](#)
- Singh, A.; Hu, R.; Goswami, V.; Couairon, G.; Galuba, W.; Rohrbach, M.; and Kiela, D. 2022. Flava: A foundational language and vision alignment model. In *Proceedings of the IEEE/CVF Conference on Computer Vision and Pattern Recognition*, 15638–15650. [4](#)
- Soomro, K.; Zamir, A. R.; and Shah, M. 2012. UCF101: A dataset of 101 human actions classes from videos in the wild. *arXiv preprint arXiv:1212.0402*. [11](#)
- Spall, J. 1992. Multivariate stochastic approximation using a simultaneous perturbation gradient approximation. *IEEE Transactions on Automatic Control*, 37(3): 332–341. [7](#), [12](#)
- Spall, J. 2000. Adaptive stochastic approximation by the simultaneous perturbation method. *IEEE Transactions on Automatic Control*, 45(10): 1839–1853. [7](#), [12](#)
- Touvron, H.; Lavril, T.; Izacard, G.; Martinet, X.; Lachaux, M.-A.; Lacroix, T.; Rozière, B.; Goyal, N.; Hambro, E.; Azhar, F.; Rodriguez, A.; Joulin, A.; Grave, E.; and Lample, G. 2023. LLaMA: Open and Efficient Foundation Language Models. *arXiv preprint arXiv:2302.13971*. [1](#)
- Tsai, Y.-Y.; Chen, P.-Y.; and Ho, T.-Y. 2020. Transfer learning without knowing: Reprogramming black-box machine learning models with scarce data and limited resources. In *International Conference on Machine Learning*, 9614–9624. PMLR. [1](#), [5](#)
- Vinod, R.; Chen, P.-Y.; and Das, P. 2020. Reprogramming language models for molecular representation learning. *arXiv preprint arXiv:2012.03460*. [1](#), [5](#)
- Wortsman, M.; Ilharco, G.; Kim, J. W.; Li, M.; Kornblith, S.; Roelofs, R.; Lopes, R. G.; Hajishirzi, H.; Farhadi, A.; Namkoong, H.; et al. 2022. Robust fine-tuning of zero-shot models. In *Proceedings of the IEEE/CVF Conference on Computer Vision and Pattern Recognition*, 7959–7971. [1](#), [5](#)
- Xiao, J.; Hays, J.; Ehinger, K. A.; Oliva, A.; and Torralba, A. 2010. Sun database: Large-scale scene recognition from abbey to zoo. In *2010 IEEE computer society conference on computer vision and pattern recognition*, 3485–3492. IEEE. [11](#)
- Yang, C.-H. H.; Tsai, Y.-Y.; and Chen, P.-Y. 2021. Voice2series: Reprogramming acoustic models for time series classification. In *International conference on machine learning*, 11808–11819. PMLR. [1](#), [5](#)
- Yen, H.; Ku, P.-J.; Yang, C.-H. H.; Hu, H.; Siniscalchi, S. M.; Chen, P.-Y.; and Tsao, Y. 2021. Neural model reprogramming with similarity based mapping for low-resource spoken command classification. *arXiv preprint arXiv:2110.03894*. [1](#), [5](#)
- Zhai, X.; Wang, X.; Mustafa, B.; Steiner, A.; Keysers, D.; Kolesnikov, A.; and Beyer, L. 2022. LiT: Zero-Shot Transfer With Locked-Image Text Tuning. In *Proceedings of the IEEE/CVF Conference on Computer Vision and Pattern Recognition (CVPR)*, 18123–18133. [4](#)
- Zhang, R.; Hu, X.; Li, B.; Huang, S.; Deng, H.; Qiao, Y.; Gao, P.; and Li, H. 2023. Prompt, Generate, Then Cache: Cascade of Foundation Models Makes Strong Few-Shot Learners. In *Proceedings of the IEEE/CVF Conference on Computer Vision and Pattern Recognition (CVPR)*, 15211–15222. [5](#)
- Zhou, K.; Yang, J.; Loy, C. C.; and Liu, Z. 2022a. Conditional prompt learning for vision-language models. In *Proceedings of the IEEE/CVF Conference on Computer Vision and Pattern Recognition*, 16816–16825. [4](#), [5](#)
- Zhou, K.; Yang, J.; Loy, C. C.; and Liu, Z. 2022b. Learning to prompt for vision-language models. *International Journal of Computer Vision*, 130(9): 2337–2348. [4](#), [5](#), [11](#)

Supplementary Material

This section contains supplementary material that provides additional details for the main paper and further experimental analysis. This section outlines the contents in the following order.

- Preliminary studies (Appendix A).
- Experimental setting (Appendix B)
- Optimizing in a gradient-free environment (Appendix C).
- Additional ablation experiments (Appendix D).

A Preliminary

We first provide a brief introduction to why visual prompting is challenging in VLMs compared to text prompting, then we discuss the mechanism of CLIP and finally discuss how visual prompting works.

A.1 Why Visual prompting is challenging in CLIP?

Images are often high-dimensional data with rich visual cues and more variability, whereas text data can be more structured and symbolic. This nature of data can affect how fast and effectively models learn and optimize, particularly if the training data is limited. By the asymmetric design of CLIP images and text encoders, their parameters influence the capacity of adapters to learn from a few data. With a large number of parameters of image encoders in CLIP as shown in Figure 3, they may require more data and time to learn complex patterns and optimize them effectively. Once pre-trained, finetuning the vision encoder fully or partially has the potential risk of failing to preserve the learned patterns.

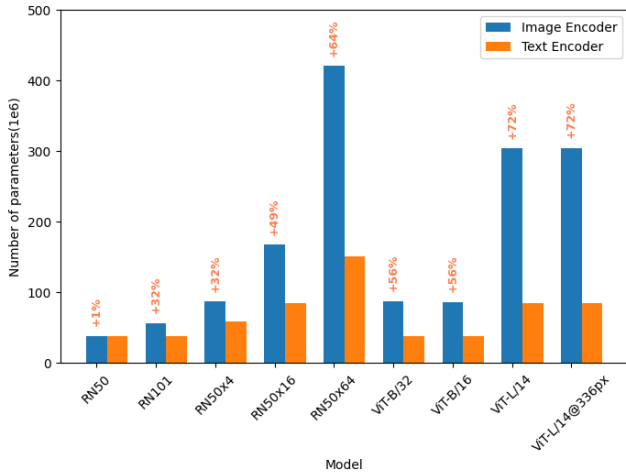


Figure 3: Number of parameters in visual and text encoders of CLIP variants (Radford et al. 2021)

Table 5 shows several learnable parameters used by different prompt learning methods. We note that, despite tuning a few parameters, language prompt learning methods such as CoOP and CoOP exhibit strong performance on few-shot learning compared to visual prompting methods (VP

Method	Prompt	Params	%CLIP
CoOP	L	2048	0.002
CoCoOP	L	35360	0.03
VP	V	69840	0.06
VPT	V	15.51 M	12.51
MaPLe	V-L	3.5 M	2.83
LaViP (Avg)	V-L	0.221 M	0.18

Table 5: Number of trainable parameters used in existing methods

and VPT). Therefore, to use the visual prompting method a new design paradigm that can promote the alignment between visio-language modalities is essential. Thereby, we propose visual prompting by leveraging the language knowledge embedded in CLIP.

A.2 CLIP

Our approach is based on CLIP which is a pre-trained vision language model that uses vision and text encoder to align the two input modalities. We evaluate LaViP using ViT-based CLIP to make a fair comparison with previous visual prompting methods. LaViP optimizes the input transformation similar to MR, therefore it can be used with vision-only models provided text embeddings and output are available. Below, we expand our discussion using ViT-based CLIP architecture.

Image Encoding: The image encoder V_{enc} consists of K transformer layers $\{V_{enc}^i\}_{i=1}^N$ input dimension of d_v and output dimension of d_{vl} . The input image is split into M fixed-size patches using a CNN layer, and then the patches are projected to linear embeddings $e_0 \in \mathbb{R}_{M \times d_v}$. The embeddings from the previous layer are passed on to the next transformer layer, along with a learnable class token c_i , and then processed sequentially through N transformer layers. Image patches are treated the same way as tokens described in [Transformer.]

For $i = 1, 2, \dots, K$

$$[c_i, E_i] = V_{enc}^i([c_{i-1}, E_{i-1}]) \quad (7)$$

The class token of the final transformer layer, c_N is projected to a shared vision-language embedding space via a ImageProj to form I_{proj} .

$$I_{proj} = \text{ImageProj}(c_k); \quad I_{proj} \in \mathbb{R}_{d_{vl}} \quad (8)$$

Text Encoding: CLIP text encoder T_{enc} consist of K transformer layers with input dimension of d_l and output dimension of d_{vl} . It first tokenizes the words to n tokens and then maps them to corresponding token embeddings $W_0 \in \mathbb{R}^{N \times d_l}$. Token embeddings from the previous layer are passed to the next transformer layer and sequentially processed through K transformer layers.

For $i = 1, 2, \dots, K$

$$[W_i] = T_{enc}^i([c_{i-2}, E_{i-1}]) \quad (9)$$

The final token of the T_{enc}^K transformer layer is projected into shared vision-language embedding space via a TextProj to form T_{proj} .

$$T_{proj} = \text{TextProj}(c_k); \quad T_{proj} \in \mathbb{R}_{d_{\text{vlt}}} \quad (10)$$

Aligning Vision and Language projection: Once the image projection I_{proj} and language projection T_{proj} are obtained, they are ℓ_2 -normalized and a similarity score ($\text{sim}(\cdot)$) is computed between the normalized projections. Both the contrastive learning processes (i.e. $V \rightarrow L$ and $L \rightarrow V$) are regarded as symmetrical operations and they are used jointly optimized during the training phase.

Zero-shot Classification For the zero-shot classification task, A set of hand-crafted prompts are used: “a photo of a $\langle class \rangle$ ” with class labels $y \in \{1, 2, \dots, C\}$. To predict the output, the $\text{sim}(\cdot)$ score between the image instance and the prompts from all the class labels is calculated. and the final score is adjusted using a scaling temperature parameter τ . The predicted output \hat{y} is the one with the highest $\text{sim}(\cdot)$ score.

$$p(\hat{y}|I_{proj}) = \frac{\exp(\text{sim}(I_{proj}, T_{proj}^{\hat{y}})/\tau)}{\sum_{i=1}^C \exp(\text{sim}(I_{proj}, T_{proj}^i))} \quad (11)$$

A.3 Revisiting Visual Prompting

Studies in NLP explored prompt learning as a method to calibre the inputs of pre-trained language models to new tasks. This motivates the use of prompt learning methods to exploit the knowledge of VLMs. Studies such as CoOP learn to adapt to the language branch, while VP learns to adapt to the vision branch.

Below, we discuss the shared rationale behind these concepts in adapting pre-trained models. Given a frozen PTM F and a target dataset $\mathcal{D} = \{(x_1, y_1), \dots, (x_k, y_k)\}$, the objective is to train a prompt learner (P) such that it generates perturbation in input space Φ_W , parameterized by learnable parameters W of P . The generated perturbation is attached to the input before feeding to the pre-trained model.

$$X_{prompted} = X + \Phi_W \quad (12)$$

During training, the P is learned to maximize the likelihood of the correct label y ,

$$\max_W \Phi_W(y|X + \Phi_W) \quad (13)$$

while the gradient updates are applied only to P . During the evaluation, the optimized parameters W^* of P are used to generate a prompt to the input and added to all the input instances.

$$X_{test} = \{x_1 + \phi_w, \dots, x_m + \phi_w\} \quad (14)$$

Given the perceptual variability of images and semantic abstraction of textual descriptions, we assert that prompt learning methods need to be adaptable for input disparity.

B Experimental Setting

B.1 Backbone Model

The primary focus of this work is directed towards achieving robust adaptation of pre-trained V-L models to diverse

downstream tasks. To conduct our experiments, we utilized the publicly available vision language model CLIP (Radford et al. 2021). To make a fair comparison with previous arts for the underlying image encoder, we chose the ViT-b/16 (Dosovitskiy et al. 2020) with dimensions $d = 512$, as our default option. Throughout the training phase, we left the entire parameters of CLIP architecture and refrained from making any structural adjustments. Our focus is solely on optimizing the prompt learner P externally.

B.2 Baseline Methods

1) *CLIP Zero-Shot(ZS)*: CLIP learns a robust shared latent space by aligning vision-language modalities through contrastive learning on nearly 400 million image-text pairs, enabling an excellent generalization ability. We aim to improve CLIP’s zero-shot performance for new tasks. 2) *VP*: (Bahng et al. 2022) proposed VP to adapt VLMs by learning pixel space prompts. It uses universal visual prompts for all images. Our algorithm expands the VP in two significant ways: 1) Creating prompts that are tailored to the input and 2) Using language supervision to enhance the synergy between the vision-language modalities.

B.3 Datasets

We follow the CoOP (Zhou et al. 2022b), VP (Bahng et al. 2022) and BlackVIP (Oh et al. 2023) and evaluate our method on different image recognition datasets across a diverse range of tasks. This includes: General images Caltech101 (Fei-Fei, Fergus, and Perona 2004); fine-grained datasets, OxfordPets (Parkhi et al. 2012), Stanford-Cars (Krause et al. 2013), Flowers102 (Nilsback and Zisserman 2008), Food101 (Bossard, Guillaumin, and Van Gool 2014), and FGVC Aircraft (Maji et al. 2013); a scene recognition dataset SUN397 (Xiao et al. 2010); an action recognition dataset UCF101 (Soomro, Zamir, and Shah 2012); a texture dataset DTD (Cimpoi et al. 2014) and a satellite image datasets EuroSAT (Helber et al. 2019b); an remote sensing scene recognition dataset RESISC45 (Cheng, Han, and Lu 2017), visual reasoning dataset CLEVR (Johnson et al. 2017), and low-resolution datasets SVHN (Netzer et al. 2011), CIFAR10 and CIFAR100 (Krizhevsky, Hinton et al. 2009). We conduct our experiments using data split provided by (Zhou et al. 2022b; Oh et al. 2023). For few-shot learning experiments, we use 16-shot for the train set, 4-shot for the validation set, and the whole test set.

B.4 Implementation Details

We use the default padding of size 28 for all our experiments based on the assessment of various padding sizes and CoOP style transformation to resize the image for CLIP. All the experiments run consist of 300 epochs run on a single NVIDIA RTX A5500 GPU, with batch size 64 for few-shot learning and 128 for full-set transfer learning. For the sake of simplicity in our few-shot transfer learning experiments, we set $r = K$ and $r_B = 32$ for P parameters when dealing with datasets featuring over 15 classes. For other datasets, we set $r = 64$ (including SUN397). In the context of base-to-domain generalization experiments, both r and r_B are set

at 32. We used SGD with a learning rate of 1.0 for all the datasets, except for StanfordCars, where we utilize a rate of 0.1. The final checkpoint is consistently used for evaluating our algorithm’s performance on the test set throughout all experiments. To ensure reproducibility in our few-shot training experiments, performance evaluation relies on calculating average accuracy across three distinct random seeds.

C Optimizing in a Gradient Free Environment

It is important to acknowledge that accessing the parameters of PTMs is not always attainable, which creates a challenge for adapting them to specific downstream tasks. Adapting in a gradient-free environment is challenging because efficient search through the parameter space is hindered, leading to potentially slow and suboptimal outcomes and reliable feedback is often limited or absent, making it hard to determine the effectiveness of learning strategies.

In this section, we provide the details of **BlackLaViP**, the gradient-free variant of LaViP. BlackLaViP utilizes *Simultaneous Perturbation Stochastic Approximation* (SPSA) algorithm (Spall 1992, 2000). SPSA approximate the gradient of high dimensional tensors by evaluating the difference between loss value under forward and backward perturbation. Given the positive decaying sequences of $a_i > 0$ and $c_i \in [0, 1]$, the gradient approximation, \hat{g} , and single-step parameter update of SPSA is described as follows:

$$\hat{g}_i(\phi_{w_i}) = \frac{L(\phi_{w_i} + c_i\Delta_i) - L(\phi_{w_i} - c_i\Delta_i)}{2c_i\Delta_i} \quad (15)$$

$$\phi_{w_{i+1}} = \phi_{w_i} - a_i\hat{g}_i(\phi_{w_i}) \quad (16)$$

where L is the loss function, $\phi_w \in \mathbb{R}^d$ is d -dimensional learnable parameters, and $\Delta_i \in \mathbb{R}^d$ is an i -th step random perturbation vector, sampled from mean-zero distributions. Utilizing two consecutive forward evaluations, the SPSA interprets the estimated gradient through the difference in model output. This unique approach empowers us to optimize BlackLaViP’s parameters ϕ_w without the reliance on backpropagation.

C.1 Implementation Details

We opt for $r = 8$ and $r_B = 32$ to effectively reduce the parameters, run all experiments for 300 epochs and evaluate the model on the last checkpoint. We have used parameters, perturbation distribution, and schedulers proposed by Black-ViP.

$$a_i = \frac{a}{(\text{step}_i + o)^\alpha}$$

$$c_i = \frac{c}{\text{step}_i^\gamma}$$

$$\text{total_}a_i\text{_steps} = \text{Total Epochs} \times \text{len}(\text{data loader})$$

Here, a_i represents the learning rate and c_i represents the perturbation scale, with specific values assigned as follows:

$$\alpha = 0.4, a = 0.01, \gamma = 0.2, o = \frac{\text{total_}a_i\text{_steps}}{\frac{\pi}{4}} \text{ and } c = 0.005$$

C.2 Base-to-Novel Generalization

Figure 4 compares BlackLaViP models in the context of generalization towards base-to-novel tasks. While it might fall short in comparison to other models in terms of performance, it is worth noting that BlackLaViP has displayed notable improvement over the CoCoOp model in the case of the EuroSAT and FGVC Aircraft datasets, and exhibits marginally less on Caltech101 and OxfordPets. Moreover, it outperforms CoOp in 6 out of 10 datasets. We consider these outcomes to be strong indicators that the incorporation of language context holds the potential to mitigate the limitations observed in previous black-box models when it comes to generalizing to unseen classes.

We would like to emphasize that the experiment was conducted with the sole intention of providing evidence for LaViP performance within a gradient-free environment. This demonstration holds substantial implications for future research, specifically in the realm of integrating language context into visual prompting for black-box training. While there might be a small loss of accuracy, the trade-off is more than justified by the advantage of achieving rapid convergence and sets a promising direction for exploring scenarios where faster convergence is of paramount importance with a small tradeoff of accuracy.

D Additional Ablation Studies

D.1 Alternate Text Prompt Templates

We evaluate the effect of context words on the performance of LaViP. Table 7 presents the effect of utilizing different text prompt templates on LaViP’s performance. We employed two distinct prompt template types across the selected datasets.

- *Base Prompt*: Use same prompt template across all datasets: “a photo of a { }”
- *Custom Prompts*: Building upon the base prompt template, integrate context-specific visual tokens, as detailed in Table 6

LaViP surpasses CLIP Zero-Shot prediction by a more significant margin when employing the base template. The inclusion of context-specific visual tokens further elevates performance. The results underscore the significance of language-grounded visual prompts in aligning vision-language modalities.

D.2 Language Integration Helps Domain Shift

We evaluate LaViP on datasets characterized by less generic concepts and varying levels of perceptual diversity. In Figure 5, we show the percentage of improvement achieved by LaViP over zero-shot CLIP. Notably, LaViP consistently

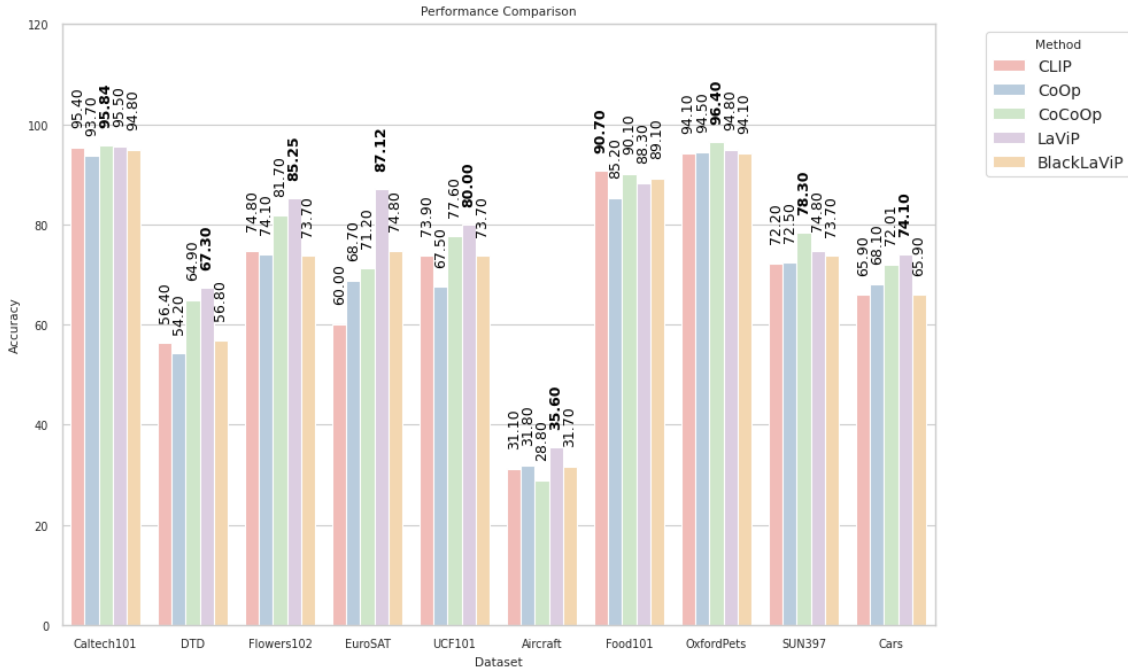


Figure 4: Performance of BlackLaViP on base-to-novel generalization. Despite trailing behind other methods, BlackLaViP outperforms CoCoOp on EuroSAT and FGVC Aircraft datasets. The best Harmonic Mean (HM) values on each dataset are bolded.

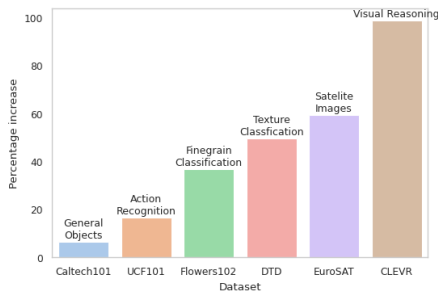


Figure 5: Classification improvement of LaViP as domain shift increase (→) from pretraining dataset of CLIP

outperforms when applied to datasets where domain shift from the pretraining dataset is more pronounced. LaViP surpasses CLIP Zero-Shot prediction by a more significant margin when employing the base template. The inclusion of context-specific visual tokens further elevates performance. The results underscore the significance of language-grounded visual prompts in aligning vision-language modalities.

D.3 Impact of Hyperparameters (a, b, r)

Table 8 presents the result obtained from 5 distinct datasets for varying r . LaViP robustly performs on these datasets when selecting r such that $r \in [16, 96]$. The effect of a, b can be studied by varying the size of padding used for vi-

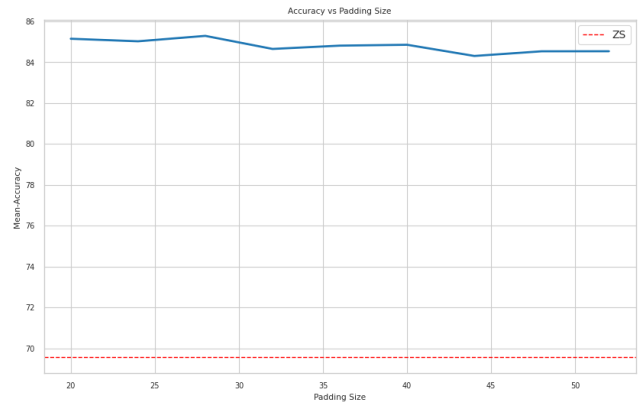


Figure 6: Average performance changes with different padding sizes. Using a moderate prompt size resulted in an overall improvement (LaViP uses $p = 28$). LaViP outperforms CLIP zero-shot prediction by a significant margin on test padding sizes.

visual prompting. Figure 6 illustrates the effect of padding size p of LaViP. The average performance of LaViP exhibits fluctuations in response to different padding sizes. It is evident that our language-grounded visual prompts consistently outperform the zero-shot CLIP approach across all tested padding sizes. This clear trend highlights the efficacy of our model. Motivated by the ability to enhance overall performance across all datasets in our experiments, we selected a

Dataset	Classes	Parameters (M)	Prompt Template
Caltech	100	0.273	“a photo of a {}.”
Pets	37	0.198	“a photo of a {}, a breed of pet.”
Cars	196	0.403	“a photo of a car model {}.”
Flowers	102	0.276	“a vibrant photo of a {}, a type of flower.”
Food	101	0.275	“a close-up photo showing delicious details of {}, a type of food.”
Aircraft	100	0.273	“a photo of an aircraft {}.”
SUN	397	0.221	“a photo showing good view of a {} location.”
DTD	47	0.210	“a photo showing fine patterns of a {}-textured surface.”
SVHN	10	0.221	“a pixelated street sign of the number {}.”
EuroSAT	10	0.221	“a photo of centered satellite top-down view {} location.”
RESISC	45	0.207	“a satellite imagery of a {} location.”
CLEVR	8	0.221	“a photo of {} colored objects.”
UCF	101	0.275	“a photo of a person actively engaged in {}.”
CIFAR10	10	0.221	“a pixelated photo of a {}.”
CIFAR100	100	0.273	“a pixelated photo of a {}.”

Table 6: Number of parameters and the text prompt template used in LaViP

Method	Caltech101	DTD	Flowers102	OxfordPets	EuroSAT	UCF101	Avg.
ZS	89.3	46.0	70.4	88.9	54.1	69.8	69.75
VP	94.2	61.9	86.9	90.2	90.8	74.2	83.03
LaViP-Base	95.0	67.7	96.2	90.3	86.0	81.1	86.05
LaViP (Ours)	95.0	68.8	96.3	91.2	86.2	81.3	86.47

Table 7: Comparison of performance when using different text prompt templates

Dataset	1	2	4	8	16	32	64	96	LaViP (Ours)
Caltech101	33.3	33.5	34.3	34.7	94.5	94.9	94.9	94.9	95.0
DTD	31.1	50.3	49.1	60.2	64.6	68.6	68.8	67.7	68.8
EuroSAT	77.2	78.7	79.9	85.0	85.7	84.0	86.1	84.3	86.1
Flowers102	44.7	49.2	26.6	88.8	93.8	95.2	96.2	96.1	96.3
OxfordPets	89.6	90.4	90.8	90.9	90.5	91.2	90.8	90.8	91.2
<i>Average</i>	55.17	60.42	56.15	71.90	85.83	86.77	87.36	86.77	87.48

Table 8: Performance of LaViP on 5 distinct datasets with varying r .

padding size of 28. Our decision also aligned with the observation previously reported by the VP.

D.4 Limitations of LaViP

Table 9 shows the performance of LaViP on low-resolution datasets compared to CLIP and VP. We hypothesize that the observed characteristic of LaViP can be attributed to the challenge of context tokens failing to establish meaningful interactions with the semantic content of the images

Method	SVHN	CIFAR10	CIFAR100	PCam
ZS	35.3	91.6	68.7	48.1
VP	60.4	73.2	49.9	73.1
LaViP (ours)	58.9	75.6	43.8	68.2

Table 9: Classification accuracy on datasets with images having low-resolution, and less semantic variation. LaViP falls short on datasets that have (a) low resolution (b) more generic concepts (c) less semantic variation.

	Source										Target													
	ImageNet	Caltech101	OxfordPets	StanfordCars	Flowers102	Food101	FGVCoAircraft	SUN397	DTD	EuroSAT	UCF101	Average	ImageNet	Caltech101	OxfordPets	StanfordCars	Flowers102	Food101	FGVCoAircraft	SUN397	DTD	EuroSAT	UCF101	Average
CoOp	71.51	93.70	89.14	64.51	68.71	85.30	18.47	64.15	41.92	46.39	66.55	63.88												
Co-CoOp	71.02	94.43	90.14	65.32	71.88	86.06	22.94	67.36	45.73	45.37	68.21	65.74												
MaPLe	70.72	93.53	90.49	65.57	72.23	86.20	24.74	67.01	46.49	48.06	68.69	66.30												
LaViP (Ours)	65.97	93.10	89.63	64.87	70.53	85.73	25.23	63.47	46.30	58.87	68.17	66.53												

Table 10: Comparison of LaViP with previous methods on cross-dataset evaluation.

due to information loss when upscaling them(SVHN, CIFAR10, CIFAR100). In cases where concept diversity is elevated (such as CIFAR10 and CIFAR100), the utilization of a single prompt template proves less effective in accommodating the wide range of contexts inherent to these concepts. Moreover, when the semantic variability of images(PCam) is diminished, the language template fails to offer meaningful context information that could facilitate improved interaction.

D.5 LaViP adaptability to CLIP variants

We evaluate to assess the compatibility of LaViP with the CNN and ViT backbones, available in CLIP. Table 12 presents the outcomes for the DTD dataset, wherein a learning rate of 0.01 was used for RN50 and RN101. The table reveals that LaViP surpasses 2 out of 3 of the tested variants, including the CNN backbone. Compared to VP, LaViP achieves an absolute gain of **8.5%** over CLIP zero shot with an optimization that is *more than 3x* faster. This result highlights that LaViP can seamlessly adapt to diverse backbone architectures while maintaining or even improving performance.

D.6 Cross-dataset Generalization

We test the cross-dataset generalization ability of LaViP by learning visual prompts on all the 1000 Imagenet (Deng et al. 2009) classes and transferring it to the remaining datasets using our Kronecker product knowledge fusion. Ta-

	Source		Target		
	ImageNet	ImageNetV2	Imagenet-S	ImageNet-A	ImageNet-R
CLIP	66.73	60.83	46.15	47.77	73.96
CoOp	71.51	64.20	47.99	49.71	75.21
Co-CoOp	71.02	64.07	48.75	50.63	76.18
MaPLe	70.72	64.07	49.15	50.90	76.98
LaViP (Ours)	65.95	61.60	47.23	48.91	83.93

Table 11: Comparison of LaViP with existing approaches in the domain generalization setting.

Method	RN50	RN101	ViT-B/16	Avg.
ZS	41.7	43.9	46.0	43.87
VP	46.0	33.3	61.9	47.07
LaViP (Ours)	42.2	46.1	68.8	52.37

Table 12: Experiment study for backbone variant of CLIP on the few-shot learning task. Classification accuracy on DTD across pre-trained backbone architectures of CLIP including the CNN and ViT.

ble 10 shows the performance comparison between LaViP, CoOp, CoCoOp and MaPLe. On the ImageNet, the performance of LaViP is suboptimal. We hypothesize this is due to the domain of ImageNet having a strong correlation with the pretraining dataset of CLIP. We used NVIDIA A100 GPU for this experiment with batch size 64 and prompt template “a cropped photo of a < class >”

D.7 Domain Generalization

To understand the domain generalization of LaViP, we transfer the ImageNet mode to various out-of-domain (OOD) datasets. Table 11 shows the comparison of domain generalization capability of LaViP compared to CLIP, CoOp, Co-CoOp and MaPLe. The performance of the ImageNet dataset impacts the performance of OOD datasets.